Phase Diagram and Structural Diversity of the Densest Binary Sphere Packings

Adam B. Hopkins, Yang Jiao, Frank H. Stillinger, and Salvatore Torquato

Phase diagram and structural diversity of the densest binary sphere packings

Adam B. Hopkins,[1] Yang Jiao,[2] Frank H. Stillinger,[1] and Salvatore Torquato[1, 2, 3, 4, 5]

[1]*Department of Chemistry, Princeton University, Princeton, New Jersey 08544, USA*
[2]*Princeton Institute for the Science and Technology of Materials,*
Princeton University, Princeton, New Jersey 08544, USA
[3]*Department of Physics, Princeton University, Princeton, New Jersey 08544, USA*
[4]*Princeton Center for Theoretical Science, Princeton University, Princeton, New Jersey, 08544, USA*
[5]*Program in Applied and Computational Mathematics,*
Princeton University, Princeton, New Jersey 08544, USA

The densest binary sphere packings have historically been very difficult to determine. The only rigorously known packings in the α-x plane of sphere radius ratio α and relative concentration x are at the Kepler limit $\alpha = 1$, where packings are monodisperse. Utilizing an implementation of the Torquato-Jiao sphere-packing algorithm [S. Torquato and Y. Jiao, Phys. Rev. E **82**, 061302 (2010)], we present the most comprehensive determination to date of the phase diagram in (α, x) for the densest binary sphere packings. Unexpectedly, we find many distinct new densest packings.

PACS numbers:

A packing is defined as a set of nonoverlapping objects arranged in a space of dimension d, and its packing fraction ϕ is the fraction of space that the objects cover. Packings of spheres can be used to describe the structures and some fundamental properties of a diverse range of substances from crystals and colloids to liquids, amorphous solids and glasses [1–3]. In particular, the densest sphere packings in d-dimensional Euclidean space $\mathbb{R}^d$, or packings with maximal packing fraction ϕ_{max}, often correspond to ground states of systems of particles with pairwise interactions dominated by steep isotropic repulsion [4–7]. Recently, packings of different sized spheres in $\mathbb{R}^3$ have been employed to model the structures of a range of materials, including, for example, solid propellants and concrete [8, 9]. The focus of the present paper is binary sphere packings, packings of spheres of two sizes, which have long been used as models for the structures of a wide range of alloys [5, 10–12].

Past efforts to identify the densest binary sphere packings have employed simple crystallographic techniques [13, 14] and algorithmic methods, *e.g.*, Monte Carlo and genetic algorithm [15, 16]. However, these methods have achieved only limited success, in part due to the very large parameter space in (α, x) of binary packings, where $\alpha \equiv R_S/R_L$ and $x \equiv \frac{N_S}{N_S+N_L}$, with R_S, N_S and R_L, N_L the respective radii and numbers of the small and large spheres in the packing, and where in the infinite volume limit $N_S + N_L \to \infty$, x remains constant. Employing traditional algorithms, difficulties result from the enormous number of steps required to escape from local minima in "energy", defined as the negative of the packing fraction.

In this work, we present the most comprehensive determination to date of the phase diagram for the densest infinite binary sphere packings. Employing an algorithmic search using an implementation of the Torquato-Jiao (TJ) linear programming algorithm [17], we identify 17 distinct alloys, including seven that were heretofore unknown, present in the densest packings over a range of (α, x) where significantly fewer were thought to be found. Previously, the alloys thought to be present for $\alpha > \sqrt{2} - 1 = 0.414213\ldots$ corresponded to structures such as the AlB_2 (hexagonal ω), $HgBr_2$, and $AuTe_2$ structures [14, 16, 18], and to two structures composed of equal numbers of small and large spheres [19]. For $\alpha \leq \sqrt{2} - 1$, the alloys thought to be present were XY_n structures of close-packed large spheres with small spheres (in a ratio of n to 1) in the interstices, *e.g.*, the NaCl packing for $n = 1$. Using the TJ algorithm, we always identify either the densest previously known alloy, or one that is denser.

The finding that such a broad array of different densest stable structures consisting of only two types of components can form without any consideration of attractive or anisotropic interactions is of significant practical importance. Our findings strongly suggest that the wide variety of atomic, molecular, and granular structures found in nature may owe much of their structural diversity to entropic (free-volume maximizing) interactions rather than only to anisotropies in nearest-neighbor bonding.

Structures, or configurations of points, can be classified as either periodic or aperiodic. Roughly defined, a *periodic* structure (packing) is one consisting of a certain number of points (sphere centers), called the *basis*, placed in a defined region of space, the *fundamental cell*, replicated many times such that the cells cover all space without any overlap between cells (or spheres). If a fundamental cell has a *minimal basis*, then a smaller cell and basis with the same periodic structure does not exist. An *aperiodic* structure has an infinite minimal basis. We use the term "alloy" in a general sense to mean a structure composed of two or more distinguishable components that are not phase-separated.

The problem of generating dense packings of nonoverlapping nonspherical particles within an adaptive fundamental cell subject to periodic boundary conditions

has been posed as an optimization problem called the adaptive-shrinking cell (ASC) scheme [20]. The TJ sphere-packing algorithm [17] is a linear-programming solution of the ASC scheme for the special case of packings of spheres with a size distribution for which linearization of the design variables, including the periodic simulation box shape and size, and impenetrability constraints, is exact. The TJ algorithm leads to strictly jammed packings of spheres with variable degrees of order, including the maximally dense packings. In a strictly jammed packing, no volume-decreasing deformation of the fundamental cell or any internal collective particle motions are possible. Consequently, maximally dense periodic packings must also be strictly jammed because otherwise the volume of the packing could be reduced [21].

Using the TJ algorithm, we have systematically surveyed the parameter space $(\alpha, x) \in [0, 1] \times [0, 1]$, omitting the rectangular area $\alpha < 0.2$, $x > 11/12$ for reasons mentioned below, to find the putative densest binary packings for all bases of up to 12 spheres. From this survey, we construct the most comprehensive determination to date of the phase diagram of the densest infinite binary packings, and the best-known lower bound on the function $\phi_{max}(\alpha, x)$, the packing fraction of the densest infinite packings of binary spheres at fixed (α, x) for the values of α in our survey; see Fig. 1. We present a detailed view of the composition of phases in Figure 2.
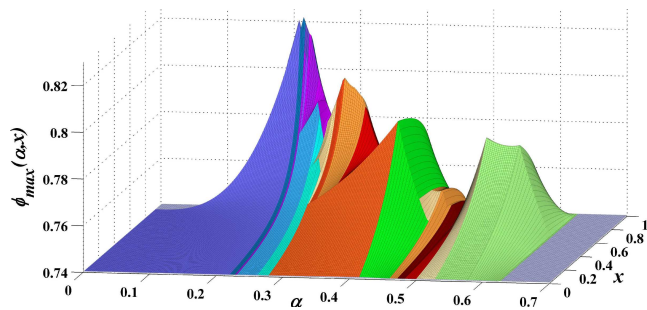

FIG. 1: (Color online) The most comprehensive determination to date of the phase diagram and maximal packing fraction surface $\phi_{max}(\alpha, x)$ of the densest infinite binary sphere packings. The highest point is $\phi_{max}(0.224744\ldots, 10/11) = 0.824539\ldots$, and all packings for $\alpha > 0.623387\ldots$ consist of two phase-separated monodisperse Barlow phases. We have excluded the rectangular region $\alpha < 0.20$, $x > 11/12$. Shadings indicate phase composition, as specified in Fig. 2.

Away from the point $(\alpha, x) = (0, 1)$, assuming that the packing fraction and composition of the generally small number of densest alloys at specified radius ratio α are known, the densest infinite packings are phase-separated combinations of alloy and/or monodisperse phases. The spheres in the monodisperse phases are packed as any of the uncountably infinite number of Barlow packings [22], *e.g.*, the well known fcc and hcp close-packed packings. However, as $\alpha \to 0$ and $x \to 1$, the number of distinct densest packings approaches infinity due to the infinite

number of XY_n and similar packings. For this reason, we exclude the region $\alpha < 0.2$, $x > 11/12$ from our study, truncating at $\alpha = 0.2$ because it is close to the maximum value $\alpha = 0.216633\ldots$ at which 11 small spheres fit in the interstices of a Barlow packing of large spheres.

When α is near the Kepler limit of unity, the densest packings consist of two phase-separated monodisperse Barlow phases of small and large spheres with packing fraction $\pi/\sqrt{18}$ [21]. This is the case in Fig. 1 for all packings with $\alpha > 0.623387\ldots$. In general, the surface is continuous and piecewise differentiable, though as $\alpha \to 0$ and $x \to 1$, the density of curves along which the surface is not differentiable approaches infinity.

In $\mathbb{R}^2$, periodic, quasicrystalline[1], directionally periodic[2] and disordered[3] structures can all be found among the putative densest binary disk packings [18, 23, 24]. We believe that all of these types of structures might be present among the densest binary sphere packings in $\mathbb{R}^3$ as well, though we do not identify quasicrystalline or disordered structures here. Due to computational constraints attributable to the scope and resolution of our survey in (α, x), we have limited our investigation to periodic packings considering all possible bases of 12 and fewer spheres. This limitation substantially increases the difficulty of identifying any aperiodic packings, which most often cannot be approximated well by a periodic packing with a basis of 12. The directionally periodic packings that we have identified are those for which no boundary cost exists between phases, *e.g.*, between AlB_2 and monodisperse phases, and these packings are therefore degenerate in density with periodic packings.

Identifying the densest packings: To identify the densest infinite binary packings in $\mathbb{R}^3$, we begin with the obvious statement that at all given (α, x), there is a densest packing that consists of a finite number of phase-separated alloy and monodisperse phases. Since we limit ourselves in this work to minimal bases of no more than 12 spheres, we must assume that all of these alloy phases can be constructed from repetitions of local structures consisting of 12 spheres or fewer. Though we recognize that this latter assumption is most likely false for some values of (α, x), we contend that for the majority of the area of the parameter space studied, it is correct.

We describe a distinct alloy as one with a unique combination of composition of spheres in its minimal basis and lattice system characterization of its fundamental

---

[1] A quasicrystal can be roughly described as an aperiodic structure that nonetheless exhibits bond orientational order in symmetries (*e.g.*, icosahedral) forbidden to periodic crystals.

[2] We describe a directionally periodic structure as an aperiodic structure that exhibits a period along at least one spatial axis but never simultaneously along all d vectors that span the space.

[3] For the purposes of this paper, a disordered structure is aperiodic but neither a quasicrystal nor directionally periodic.

FIG. 2: (Color online) Phase diagram in (α, x), excluding the region $\alpha < 0.2$ and $x > 11/12$, of the densest-known infinite binary sphere packings considering periodic packings with minimal bases of 12 or fewer spheres.

cell. This is a more encompassing characterization than that applied in Ref. [18], where periodic alloys in the densest binary disk packings were classified by composition and the numbers of small and large sphere contacts in the fundamental cell. For example, the distinct alloy with six small and one large sphere in its minimal basis and fundamental cell belonging to the triclinic lattice system exhibits a wide range of contact networks over the range $0.292 \leq \alpha \leq 0.344$ when it appears in the densest packings. To illustrate this point, we have divided this alloy into three subcategories, $(6\text{-}1)_8$, $(6\text{-}1)_6$, and $(6\text{-}1)_4$, where the subscript indicates the number of large sphere contacts per large sphere, as depicted in the detailed phase diagram (Fig 2). We note that the alloy could be further subdivided by the numbers of small-small and large-small contacts.

The boundaries between phases are negligible in the infinite volume limit, and so the packing fraction of a collection of phase-separated monodisperse and β distinct alloy phases can be written as,

$$\phi(\alpha, x) = \frac{\frac{4\pi}{3}\left((1-x)R_L^3 + xR_S^3\right)}{xC_B^S + (1-x)C_B^L + \sum_{i=1}^{\beta} x_i^L\left(\frac{C_i}{L_i} - \frac{S_i}{L_i}C_B^S - C_B^L\right)},\tag{1}$$

with C_B^S and C_B^L the volume per sphere, respectively, in a close-packed Barlow packing of small and large spheres, x_i^L the relative fraction of large spheres distributed in alloy phase i, and C_i the volume of a fundamental cell of alloy phase i containing L_i large and S_i small spheres. The constraints $x_i^L \geq 0$, $\sum_{i=1}^{\beta} x_i^L \leq 1-x$, and $\sum_{i=1}^{\beta}(S_i/L_i)x_i^L \leq x$ must be valid due to conservation of total particle numbers.

To find the densest packing $\phi_{max}(\alpha, x)$ from among β alloy and two close-packed monodisperse phases, Eq. (1) must be maximized. This is accomplished by treating the aforementioned $\beta + 2$ constraints and the summation term in the denominator of Eq. (1) as a linear programming problem where the objective is to minimize

the summation. From this postulation, it can be proved [25] that there is always a densest binary packing consisting of no more than two phase-separated phases, though it may be degenerate in density with packings consisting of more than two phases or with mixed phase packings.

Using Eq. (1) and considering a fixed value of α, the densest infinite binary packings constructed from binary alloys with bases of 12 or fewer spheres can be found for all values of x. This only requires knowing the densest packings in a fundamental cell for combinations of positive integer S_i and L_i such that $S_i + L_i = 2, 3, \ldots, 12$. Employing the TJ algorithm, we have solved these problems (putatively) to accuracy of about 10^{-4} in ϕ for α spaced 0.025 apart, and on a finer grid with α spaced about 0.0028 apart for certain values of S_i and L_i where particularly dense packings were identified.

Figure 2 is our determination of the phase diagram, described with heretofore unattained accuracy, for the densest infinite binary sphere packings considering periodic packings with minimal bases of 12 or fewer spheres. In the diagram, the seven previously unrecognized distinct alloys are described according to the composition of their minimal basis, e.g., (6-6) for a packing with 6 small and 6 large spheres per fundamental cell. In Fig. 2, the points (lines) where the composition of phase-separated phases changes from alloy plus monodisperse packing of small spheres to the same alloy plus large spheres are not drawn. Additionally, when only one alloy is listed, it is assumed that the densest packing consists of a monodisperse phase and an alloy phase, except at points such that $x = S_i/(S_i + L_i)$, with S_i and L_i the respective numbers of small and large spheres in the alloy phase listed, where only the alloy phase is present.

We briefly describe the 17 distinct alloys here, leaving the detailed descriptions for a later work [25]. The XY_n alloys are present for $n = 1, 2, 4, 8, 10$ and 11. In these packings, the large spheres are close-packed Barlow packings, and the small spheres are inside the inter-

stices as rattlers, movable but caged spheres, except for at "magic" [18] α where they are jammed. Additionally, for $n = 2$, 4, 8 and 10, there are XY_n alloys for α greater than the magic radius ratios. These packings consist of large spheres arranged as in a Barlow packing but not in contact, with interstitial jammed small spheres arranged as was the case for the magic α.

The AlB_2 alloy is well known, and the $HgBr_2$ and $AuTe_2$ alloys, described in another work [16], have, respectively, four small and two large and two small and one large spheres in their fundamental cells. The alloys belong to the orthorhombic and monoclinic lattice systems, respectively. The alloy listed as (2-2)* exhibits the same packing fraction (error of less than 10^{-4}) over the range $0.480 \leq \alpha \leq 0.497$ where it appears in the densest packings as the alloy described in Ref. [19] as "Structure 2", though "Structure 2" has four small and four large spheres in its fundamental cell. Due to the precise agreement of packing fractions, we postulate that the two alloys may be the same or have materially negligible differences over the range $0.480 \leq \alpha \leq 0.497$.

There are two alloys, (11-1) and (10-1), that are similar to the XY_{11} and XY_{10} packings except that their fundamental cells belong to the tetragonal and rhombohedral lattice systems, respectively, as opposed to cubic. The $(6\text{-}1)_{10}$ alloy can be described as an orthorhombic body-centered packing of large spheres, each with ten large-large sphere contacts, with four small spheres on each face. The alloy subdivided as $(6\text{-}1)_8$, $(6\text{-}1)_6$, and $(6\text{-}1)_4$ in Fig. 2 is similar but with a skewed fundamental cell belonging to the triclinic lattice system.

Over the range $0.414 < \alpha < 0.457$ where the (6-6) alloy appears in the densest packings, we have found that in simulation, increasing the basis from one small and one large spheres up to six small and six large spheres in a one-to-one ratio results in alloys with increasing packing fraction. The simulations with four large and four small spheres in the fundamental cell produce an alloy with packing fractions that agree (error of less than 10^{-4}) with those of "Structure 1" described in Ref. [19]. The (5-2) alloy is arranged as offset square lattice layers of large spheres with small spheres in between; the alloy belongs to the monoclinic lattice system. The (7-3) alloy fundamental cell belongs to the orthorhombic lattice system. The alloy is similar to three adjacent fundamental cells of an AlB_2 packing with one extra small sphere inserted.

Our determination of the phase diagram (Figs. 1 and 2) describes an unexpected diversity in the densest binary sphere packings, with 17 distinct alloys present. One implication of these findings is that entropic (free-volume maximizing) particle interactions contribute to the structural diversity of mechanically stable and ground-state structures of atomic, molecular, and granular solids. Additionally, the structures we have identified can be useful as known points of departure when investigating experimentally the properties of binary solids composed of par-

ticles that exhibit steep isotropic pair repulsion. Finally, our results serve as crucial references states for studies of corresponding disordered binary sphere packings.

We have carried out a comprehensive study of the densest infinite binary sphere packings at high resolution in α and x, leading to the discovery employing the TJ algorithm of many heretofore unknown structures. Though we have limited ourselves to minimal bases of 12 or fewer spheres, the discovery of the (7-3), (6-6), and (5-2) alloys suggests that periodic structures with minimal bases larger than 12, further directionally-periodic, quasicrystalline and disordered structures might be present among the densest packings. Additionally, it is possible that densest packings have a relation to the structures of glassy binary sphere solids and/or to those of binary sphere liquids near the freezing point. In future work, we will investigate these possibilities.

[1] S. Torquato, *Random Heterogeneous Materials* (Springer, 2002).

[2] P. M. Chaikin and T. C. Lubensky, *Principles of Condensed Matter Physics* (Cambridge, 1995).

[3] A. B. Hopkins, F. S. Stillinger, and S. Torquato, Phys. Rev. E **83**, 011304 (2011).

[4] G. L. Pollack, Rev. Mod. Phys. **36**, 748 (1964).

[5] J. V. Sanders, Phil. Mag. A **42**, 705 (1980).

[6] P. Bartlett, R. H. Ottewill, and P. N. Pusey, Phys. Rev. Lett. **68**, 3801 (1992).

[7] M. Amsler and S. Goedecker, J. Chem. Phys. **133**, 224104 (2010).

[8] M. Kolonko, S. Raschdorf, and D. Wäsch, Gran. Matt. **12**, 629 (2010).

[9] F. Maggi, S. Stafford, T. L. Jackson, and J. Buckmaster, Phys. Rev. E **77**, 046107 (2008).

[10] W. Hume-Rothery, R. E. Smallman, and C. W. Haworth, *The Structure of Metals and Alloys, 5th ed.* (Metals and Metallurgy Trust, 1969).

[11] S. K. Sikka, Y. K. Vohra, and R. Chidambaram, Prog. Mat. Sci. **27**, 245 (1982).

[12] M. D. Eldridge, P. A. Madden, and D. Frenkel, Nature **365**, 35 (1993).

[13] T. S. Hudson and P. Harrowell, J. Phys. Chem. B **112**, 8139 (2008).

[14] M. J. Murray and J. V. Sanders, Phil. Mag. A **42**, 721 (1980).

[15] J. K. Kummerfeld, T. S. Hudson, and P. Harrowell, J. Phys. Chem. B **112**, 10773 (2008).

[16] L. Filion and M. Dijkstra, Phys. Rev. E **79**, 046714 (2009).

[17] S. Torquato and Y. Jiao, Phys. Rev. E **82**, 061302 (2010).

[18] C. N. Likos and C. L. Henley, Phil. Mag. B **68**, 85 (1993).

[19] G. W. Marshall and T. S. Hudson, Contr. Alg. Geo. **51**, 337 (2010).

[20] S. Torquato and Y. Jiao, Nature **460**, 876 (2009).

[21] S. Torquato and F. H. Stillinger, Rev. Mod. Phys. **82**, 2633 (2010).

[22] W. Barlow, Nature **29**, 186 (1883).

[23] F. Toth, *Regular Figures* (Macmillan, 1964).

[24] P. W. Leung, C. L. Henley, and G. V. Chester, Phys. Rev. B **39**, 446 (1989).

[25] A. B. Hopkins, F. H. Stillinger, and S. Torquato, manuscript in preparation.